ELSEVIER

Nuclear Instruments and Methods in Physics Research B 175–177 (2001) 382–387

NIM B
Beam Interactions with Materials & Atoms

www.elsevier.nl/locate/nimb

Determination of solid-state sulfidation mechanisms in ion-implanted copper

J.C. Barbour *, J.W. Braithwaite, A.F. Wright

Sandia National Laboratories, MS 1415, Org. 01112, Albuquerque, NM 87185-1415, USA

Abstract

Ion-beam irradiation and ion implantation were used to evaluate the influence of point defects and alloying elements on the sulfidation rate of copper films in atmospheric environments containing H_2S. Low-energy ions from an oxygen plasma were used to grow thin metal oxide passivation layers on Cu films that were subsequently irradiated and exposed to sulfidizing environments (50–600 ppb H_2S in air with 0.5–85% relative humidity). The type of oxide proved to be important in that a CuO layer essentially prevented sulfidation whereas a Cu_2O layer permitted sulfidation. For the native copper oxide (Cu_2O), density-functional theory modeling of Cu divacancy binding energies suggested that alloying with In or Al would cause vacancy trapping and possibly slow the rate of sulfidation. This finding was then experimentally verified for an In-implanted Cu film. A series of marker experiments using unalloyed Cu showed that sulfidation proceeds by solid-state transport of Cu from the substrate through the Cu_2S product layer.

PACS: 61.72.Tt; 61.72.Vv; 61.72.Ww; 61.72.Yx
Keywords: Implantation; Irradiation; Corrosion mechanisms; Copper sulfidation; Density-functional theory

1. Introduction

Ion implantation has been used in a number of previous corrosion studies but generally the focus has been to alloy the surface to vary the corrosion susceptibility for a given base metal (e.g. steels, Al, Ti, see [1–3]). Less work has involved the application of ion beam modification to determine mechanisms of corrosion [4,5]. The study described in this paper is the first to use ion beams specifically to determine the influence of solid-state transport process on the characteristics of atmospheric copper sulfidation. Solid-state diffusion of vacancies in Cu, Cu_2O, CuO and Cu_2S may be important processes in determining the kinetics of Cu sulfidation. The findings from this study have been achieved by combining solid-state measurements of sulfidation kinetics with density-functional theory (DFT) modeling. In this latter activity, the local density approximation is used to model the energetics of vacancy diffusion and trapping in the various materials of interest. Specific topics addressed in this study include the role

* Corresponding author. Tel.: +1-505-844-5517; fax: +1-505-844-1197.
E-mail address: jcbarbo@sandia.gov (J.C. Barbour).

0168-583X/01/$ - see front matter
PII: S0168-583X(00)00682-0

point defects and vacancy traps have on Cu diffusivity through the oxide and sulfide layers and the resultant relative rate of copper sulfidation. The effect of varying oxide type through ion irradiation was also examined. In this work, ion beams introduce both vacancies and alloying elements to permit the effects of sulfidation to be examined and compared with predicted behavior from the DFT calculations.

2. Experiment

Copper films were electron beam evaporated at a rate of 0.15–0.3 nm/s onto SiO_2-coated Si wafers at 35–42°C. The evaporation source material was 99.9999 at.% Cu. The base pressure of the sample preparation system was 2×10^{-8} Torr. These samples were then oxidized by either using energetic O_2^+ ions from an electron cyclotron resonance (ECR) oxygen plasma at temperatures varying from 35°C to 60°C or by exposure to air at room temperature. The copper films exposed to an ECR plasma formed a thin, dense surface-oxide layer that could be ion irradiated with different ion species and fluences. The O_2^+ ions in the ECR plasma, with a mean energy of approximately 30 eV, were generated using 100 W of 2.45 GHz microwave power and a magnetic field of 875 G, forming the ECR resonance condition upstream from the deposition chamber. The plasma offered a method to controllably form CuO at the surface, ≈4.0 nm thick, in a clean UHV environment. The effects of ion irradiation on the ECR-oxidized layer were examined as a function of 200 keV Cu^+ fluence. After ECR plasma oxidation, the sample surface was examined in situ using X-ray photoelectron spectroscopy (XPS), stimulated with Al Kα X-rays, in order to identify the type of oxide(s) present. The Cu $2p_{3/2}$ and O 1s core level spectra were measured as well as the Cu LMM Auger spectrum.

The copper films were also implanted with different ion species to examine the effects of surface alloying on the sulfidation rate and specifically to look for changes in the rate due to vacancy trapping. Implanted species included D, O and In. Samples were ion implanted with either In or O to form a uniform concentration profile of 0.5 at.% up to a depth of 150 nm. Another set of samples was implanted with 13 keV D to form an implantation profile centered at a depth of 107 nm with a FWHM of 120 nm. The ion implantation energies and fluences are given in Table 1. The treated copper samples were sulfidized for various times in an ambient temperature atmosphere (∼ 23–25°C) containing 50–600 ppb H_2S, 0.5–80% relative humidity (RH), and air. Following exposure, the morphology and composition of the sulfide layer were examined using scanning electron microscopy and Rutherford backscattering spectrometry (RBS). The total thickness of Cu_2S layer after H_2S exposure was measured using ion beam analysis of broad area samples.

3. Results and discussion

Fig. 1 is the XPS spectrum for the Cu $2p_{3/2}$ region from a Cu film that was exposed to an ECR O_2 plasma for 10 min at 50–60°C (solid line) and for the same sample after irradiation with 200 keV Cu^+ ions to a fluence of 1.6×10^{15} Cu/cm^2. The spectrum for a similar sample that was oxidized in

Table 1
Ion implantation conditions for examining surface alloying effects on sulfidation

	Species		
Implant #	D	O	In
1	13 keV, 5.5×10^{15} cm^{-2}	95 keV, 5×10^{15} cm^{-2}	600 keV, 4×10^{15} cm^{-2}
2		45 keV, 1×10^{15} cm^{-2}	300 keV, 8×10^{14} cm^{-2}
3		20 keV, 8×10^{14} cm^{-2}	125 keV 8×10^{14} cm^{-2}
4			30 keV, 2.5×10^{14} cm^{-2}

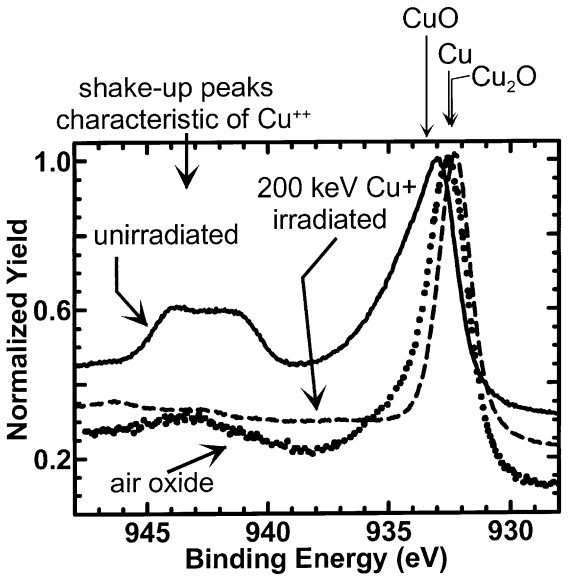

Fig. 1. Cu $2p_{3/2}$ XPS spectrum taken using Al Kα X-rays for different Cu-oxides: air-formed, ECR oxidized, and ECR-oxidized and irradiated with 200 keV Cu ions.

air for four days is also shown in this figure. The Cu $2p_{3/2}$ peak positions for CuO, Cu and Cu_2O are marked with arrows at the top of the figure. In addition, the broad shake-up peak (at 940–945 eV) is also indicated, which is a characteristic peak of Cu in the +2 oxidation state. Analysis of these spectra combined with the O 1s and Cu LMM Auger transitions (not shown) demonstrated that the surface of the ECR oxidized sample is primarily composed of CuO (with possibly a small amount of $Cu(OH)_2$) whereas the native air-oxide is Cu_2O with a minor amount of Cu in a +2 oxidation state. Strikingly, the irradiated CuO surface was completely converted from a +2 oxidation state to a +1 state (no visible sign of a shake-up peak and a significant shift in the primary peak at 932.5 eV).

The structure of Cu_2O is a fairly open, simple cubic structure with 2 formula units per cell. It has a density of 6.1 g/cm^3 and a molecular weight of 143.09 g/mol. In comparison, the structure of CuO is a more compact monoclinic crystal with 4 formula units per cell and a density of 6.51 g/cm^3, while having a molecular weight of only 79.55 g/mol. Thus, it is expected that the barrier for diffusion through the more compact CuO structure would be considerably higher.

A TRIM [6] calculation showed that the Cu ion average range (R_p) is 58 nm (with a ΔR_p of 25 nm) which is much greater than thickness of the oxide (≈4 nm). Therefore, the compositional changes in the oxide layer from the tail of the Cu implant are expected to be minimal. However, the level of points defects for this fluence is high, increasing with depth in the oxide layer up to about 3 displacements per atom (dpa). Such a high level of defects causes a complete reduction in the oxidation state of Cu in the oxide from Cu^{++} to Cu^{+}. It is reasonable to assume that Cu would need to migrate in from the substrate to accommodate this complete change in the oxidation state. The existence of such a process would then require a high mobility of Cu into and through the highly defected oxide.

By comparing the sulfidation behavior of the CuO/Cu to the Cu_2O/Cu, a better understanding was obtained of the solid-state diffusion processes involved in the sulfidation of copper. Samples with oxidized surfaces that were completely Cu_2O were compared to those with surfaces that were completely CuO. After exposure for 5.5 h at 24°C to a 65% relative humidity air atmosphere containing 600 ppb H_2S, the CuO-covered sample showed no visible (or measurable by ion beam analysis) sign of sulfidation whereas the sample with a Cu_2O layer formed a Cu_2S layer with ≈32 nm thickness (Fig. 2, RBS spectrum).

Modeling calculations were performed to determine the single-site Cu-vacancy formation energy and the split-vacancy formation energy in Cu_2O. These calculations employed the Vienna Ab Initio Simulation Package (VASP) [7–10] and utilized ultrasoft pseudo-potentials [11] within the framework of the Kohn–Sham formulation of density-functional theory [12–14]. The split vacancy is one formed when a Cu atom is removed from the Cu sub-lattice and the crystal is allowed to relax to an equilibrium state (at $T = 0$ K) such that a neighboring Cu atom relaxes into an interstitial site (approximately half way toward the vacant site). The net result of this relaxation is to split the single vacancy between the two sites adjacent to the relaxed Cu in the interstitial site. The

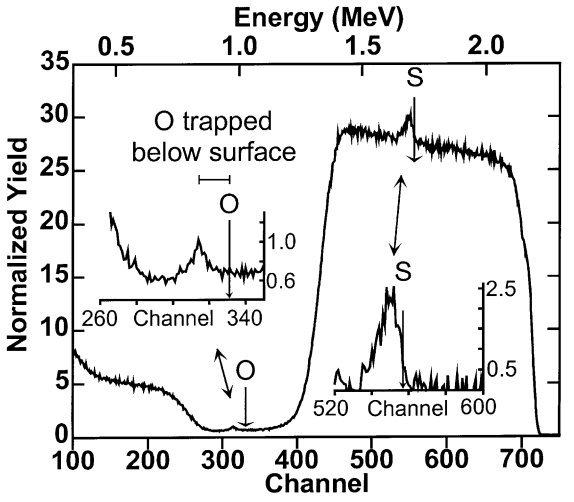

Fig. 2. RBS spectrum from an ECR-oxidized sample implanted with 200 keV Cu to a fluence of 1×10^{15} Cu/cm^2 and then sulfidized for 5.5 h in a 65% RH air environment containing 600 ppb H_2S. The RBS spectrum was collected using 2.8 MeV He ions incident at 45° from the surface normal and a scattering angle of 164°.

split-vacancy formation energy is approximately 0.10 eV lower than the single-vacancy formation energy (depending slightly on the charge state of the vacancy). The barrier for Cu-vacancy diffusion through the split-vacancy site is ≈0.3 eV whereas the barrier for diffusion through the single-vacancy site (no relaxation allowed) is ≈0.75 eV. In either case, the barrier for Cu-vacancy diffusion through Cu_2O is small suggesting that Cu should be relatively mobile in and through Cu_2O (especially through the split-vacancy site). Transmission electron microscopy (TEM) of ECR-oxidized copper [15] revealed that the grain sizes for both CuO and Cu_2O ranged from 10 to 100 nm. Therefore, with such small but equivalent grain sizes for the two oxides, if copper sulfidation were primarily dependent upon grain boundary diffusion, then similar sulfidation rates should have been found for the CuO and Cu_2O samples.

Combining the results from the DFT calculations, the TEM analysis, and the experimental results suggest that the sulfidation rate is slowed or completely suppressed by increasing the barrier to Cu-vacancy diffusion. Another possible finding based on the experimental results is that if the sulfidation process depends on supplying copper to the surface, then lattice diffusion is as important if not more important than grain-boundary diffusion.

Further examination of the oxygen and sulfur signals in the RBS spectrum of Fig. 2 indicates only two possible reaction processes for the formation of the Cu_2S layer on the surface. This spectrum was collected from a sample that was ECR-oxidized for 19 min at 75°C, forming a 9.4 nm thick CuO layer. The sample was implanted with 200 keV Cu and sulfidized for 5.5 h. Further experimental details are given in the figure caption. An enlarged view of the S signal (with background subtracted) and the O signal are shown as insets in Fig. 2. Arrows in these insets indicate the positions for the surface peaks of the S and O, respectively. The sulfur clearly resides at the surface and extends in depth whereas the O signal is below the surface peak position, demonstrating that the O is trapped below the surface Cu_2S layer. Either Cu vacancies have diffused through the oxide to form a surface sulfide layer, thereby burying the oxide layer, or the surface oxide layer reacted directly to form the sulfide, releasing the O and "snowplowing" it below the sulfidized layer. The latter possibility requires the diffusion of sulfur (or S vacancies) through the sulfide layer to supply the sulfidation reaction at the Cu_2O/Cu_2S interface.

A series of inert-marker experiments were performed to confirm which of the two candidate species actually diffuses through the combined oxide/sulfide layer. These experiments were performed using bulk polycrystalline Cu substrates possessing a native Cu_2O surface. The samples were exposed for 4 h at room temperature to an 80% RH air environment containing 150 ppb H_2S that formed an initial Cu_2S layer approximately 135 nm thick. An Au marker layer was then deposited to a thickness equivalent to 2 nm. However, for such a thin layer, the Au forms a low density of small patches (depicted schematically in Fig. 3), each with a thickness greater than 2 nm. The presence of this patchy Au layer was confirmed using a scanning electron microscope with backscattered electron imaging to highlight the elemental contrast between Au and Cu. Many RBS spectra were collected as a function of sulfidation time, but for clarity, only four spectra are

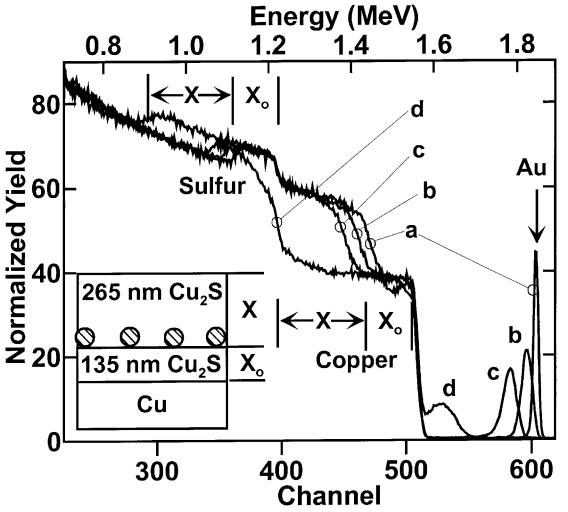

Fig. 3. RBS spectra collected from the marker-experiment samples using 2 MeV He^+ ions incident along the sample normal and a scattering angle of 164°. The Au patches, indicated schematically in the inset, were used as markers to determine the dominant moving species.

shown in Fig. 3: (a) initial 4-h sulfidation with Au marker on top, (b) sample (a) + additional 4-h sulfidation, (c) sample (a) + additional 12-h sulfidation, and (d) sample (a) + additional 103-h sulfidation. The "motion" of the Au marker to continually greater depths below the growing Cu_2S layer clearly identifies Cu vacancies are the fastest moving species through the oxide and sulfide layers. A schematic diagram depicting the composition depth profile determined from spectrum (d) is shown in the inset in Fig. 3. For each of the other spectra analyzed, the thickness of the layer X_0 was 135 nm that equaled the initial sulfide thickness before depositing the Au markers. Only for the final sulfidation did the layer X_0 begin to thicken slightly. This thickening corresponds to evidence in the gas flow analysis during the final sulfidation, suggesting that the sulfide layer formed microcracks which permitted the sulfidizing species to reach the Cu substrate, without diffusing through the solid state. The fact that the thickness of layer X_0 remained constant and all sulfide growth occurred above the markers for the other analyses proves that the sulfidizing species are not diffusing through the solid to react at the oxide/sulfide interface, but rather the Cu vacancies are the primary moving species.

A preliminary finding of this study described earlier and based on a comparison of the relative sulfidation behavior of CuO/Cu and Cu_2O/Cu samples was that the sulfidation rate can be slowed by increasing the barrier to Cu-vacancy diffusion. This concept was further tested using ion implantation to form surface alloys that could serve as Cu-vacancy traps and thereby slow the sulfidation rate. Again, DFT was employed to calculate the binding energy of a Cu divacancy to either an Al or In substitutional atom sitting on a Cu lattice site in Cu_2O. A divacancy trap was considered in order to maintain charge neutrality for the substitutional divacancy complex. The results of these calculations show strong trapping (binding) energies for both Al and In substitutional atoms: $(Al_{Cu}+2V_{Cu})^0 = 3.19$ eV with respect to unbound Al^{2+}_{Cu} and $2V^{1-}_{Cu}$, and $(In_{Cu}+2V_{Cu})^0 = 1.53$ eV with respect to unbound In^{2+}_{Cu} and $2V^{1-}_{Cu}$. Thin film, ECR-oxidized Cu samples were implanted with In, O and D according to the details shown in Table 1. These samples were all sulfidized in a 50 ppb H_2S, 80% RH, air environment at 35°C for 5 h. The amount of sulfur uptake was measured using RBS with a 2.8 MeV He^+ beam incident normal to the sample surface and with a scattering angle of 164°. The sulfur signal for these samples is given in Fig. 4 with the background stripped-off: (a) In-implanted sample, (b) O-implanted sample, and (c) D-implanted sample. A control sample with only a native Cu_2O on the surface gave a spectrum equivalent to the O-implanted sample and is not shown to maintain clarity in the figure. The surface peak position for sulfur is indicated in the figure with an arrow. These peaks are barely resolved and somewhat noisy as a result of the large Cu background signal subtracted from below them. Therefore, each signal was simply integrated to give the areal density of sulfur: (a) $3.6 \times 10^{16} \pm 0.6 \times 10^{16}$, (b) $4.8 \times 10^{16} \pm 0.7 \times 10^{16}$, and (c) $5.9 \times 10^{16} \pm 0.8 \times 10^{16}$ S/cm^2. These results validate the ab initio calculation that the In is effective at slowing the sulfidation reaction, presumably by trapping vacancies, in comparison to the O-implanted sample and control sample. Further, the D implantation, which produced far less

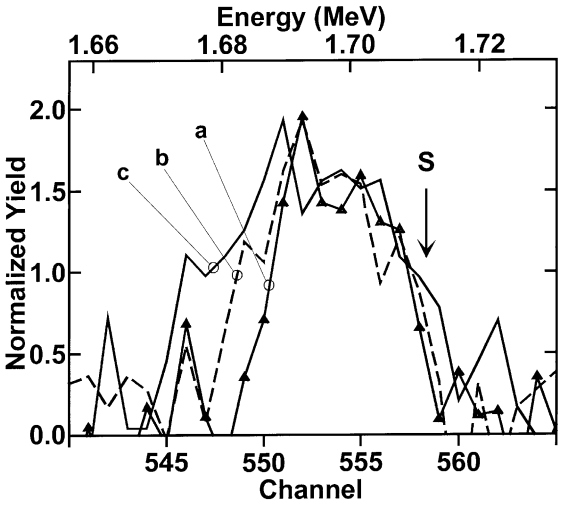

Fig. 4. Sulfur signals determined from RBS analysis with a 2.8 MeV He^+ beam incident normal to the sample surface and with a scattering angle of 164°: (a) In implanted, (b) O implanted, and (c) D implanted. The large Cu background signal was subtracted from below the S peak for each of these spectra.

damage in the oxide layer than did the In implant, had a 65% greater sulfidation rate than did the In-implanted sample. This latter result suggests that the presence of hydrogen species in the Cu can either increase the Cu-vacancy permeability or enhance the surface reaction rate.

4. Summary

Ion implantation and ion-beam irradiation has been used in this study for the first time to determine the influence of solid-state transport processes on the behavior of copper in atmospheric-sulfidizing environments. Processes involving diffusion in Cu, Cu_2O, CuO and Cu_2S were considered. In combination with solid-state measurements of sulfidation kinetics and DFT calculations, several findings resulted including (1) the role point defects and vacancy traps have on Cu diffusivity through the oxide and sulfide layers and the resultant effect on sulfidation kinetics, (2) the effect of the type of surface oxide, and (3) the identification of the dominant species that diffuses through the sulfide product layer. For the native copper oxide (Cu_2O), the importance of vacancy trapping on slowing the rate of sulfidation was predicted and experimentally verified. The type of oxide proved to be important in that a CuO layer essentially prevents sulfidation whereas a Cu_2O layer permits sulfidation. Finally, solid-state transport of Cu from the substrate through the Cu_2S product layer is the primary mass transport process.

Acknowledgements

We thank Ken Minor for performing the ion implantation, Dan Buller for assistance with the ion beam analysis, and Sam Lucero for assistance with sulfidation exposures. Sandia is a multiprogram laboratory operated by Sandia Corporation, a Lockheed Martin Company, for the US Department of Energy under Contract DE-AC04-94AL85000.

References

[1] C.M. Rangel, T.I.C. Paiva, Surf. Coat. Tech. 83 (1996) 194.
[2] B.D. Sartwell, P.N. Natishan, E.P. Donovan, S.N. Bunker, A.J. Armini, Surf. Coat. Tech. 83 (1996) 183.
[3] H. Schmidt, G. Stechmesser, J. Witte, M. Soltani-Farshi, Corrosion Sci. 40 (1998) 1533.
[4] N.G. Thompson, B.D. Lichter, B.R. Apleton, E.J. Kelly, C.W. White, in: C.M. Preece, J.K. Hirvonen (Eds.), Ion Implantation Metallurgy, The Metallurgical Society of AIME, Warrendale, PA, 1980, p. 181.
[5] G. Dearnely, in: S.T. Picraux, E.P. EerNisse, F.L. Vook (Eds.), Applications of Ion Beams to Metals, Plenum, New York, 1974, p. 63.
[6] J.F. Ziegler, J.P. Biersack, in: The Stopping and Range of Ions in Solids, Pergamon, New York, 1985 (see also TRIM92 computer code by J.F. Ziegler, IBM Yorktown Heights, New York).
[7] G. Kresse, J. Hafner, Phys Rev. B 47 (1993) 558.
[8] G. Kresse, J. Hafner, Phys Rev. B 49 (1994) 14251.
[9] G. Kresse, J. Furthmüller, Comput. Mater. Sci 6 (1996) 15.
[10] G. Kresse, J. Furthmüller, Phys. Rev. B 54 (1996) 11169.
[11] D. Vanderbilt, Phys. Rev. B 41 (1990) 7892.
[12] W. Kohn, L.J. Sham, Phys. Rev. 140 (1965) A1133.
[13] D.M. Ceperley, B.J. Alder, Phys. Rev. Lett. 45 (1980) 566.
[14] J.P. Perdew, A. Zunger, Phys. Rev. B 23 (1981) 5048.
[15] Michael Campin, New Mexico State University, private communication.